

# Recent theoretical progresses on charmonium production in PANDA

Jun-Zhang Wang (王俊璋)

Lanzhou University



Institute of Modern Physics, Chinese Academy of Sciences, December 13, 2019

# Outline

- Charmonium and charmoniumlike XYZ states
- Charmonium production in the low energy proton-antiproton collision.
- Predictions of the  $p\bar{p} \rightarrow \psi(3770)\pi^0$  and  $p\bar{p} \rightarrow \psi(3686)\pi^0$  reaction
- Predictions of the  $p\bar{p} \rightarrow Y(4220)\pi^0$  reaction

## Experimentally established charmonium states

J.Z.Wang, D.Y.Chen, X.Liu and T.Matsuki,  
Phys. Rev. D 99, no. 11, 114003 (2019)

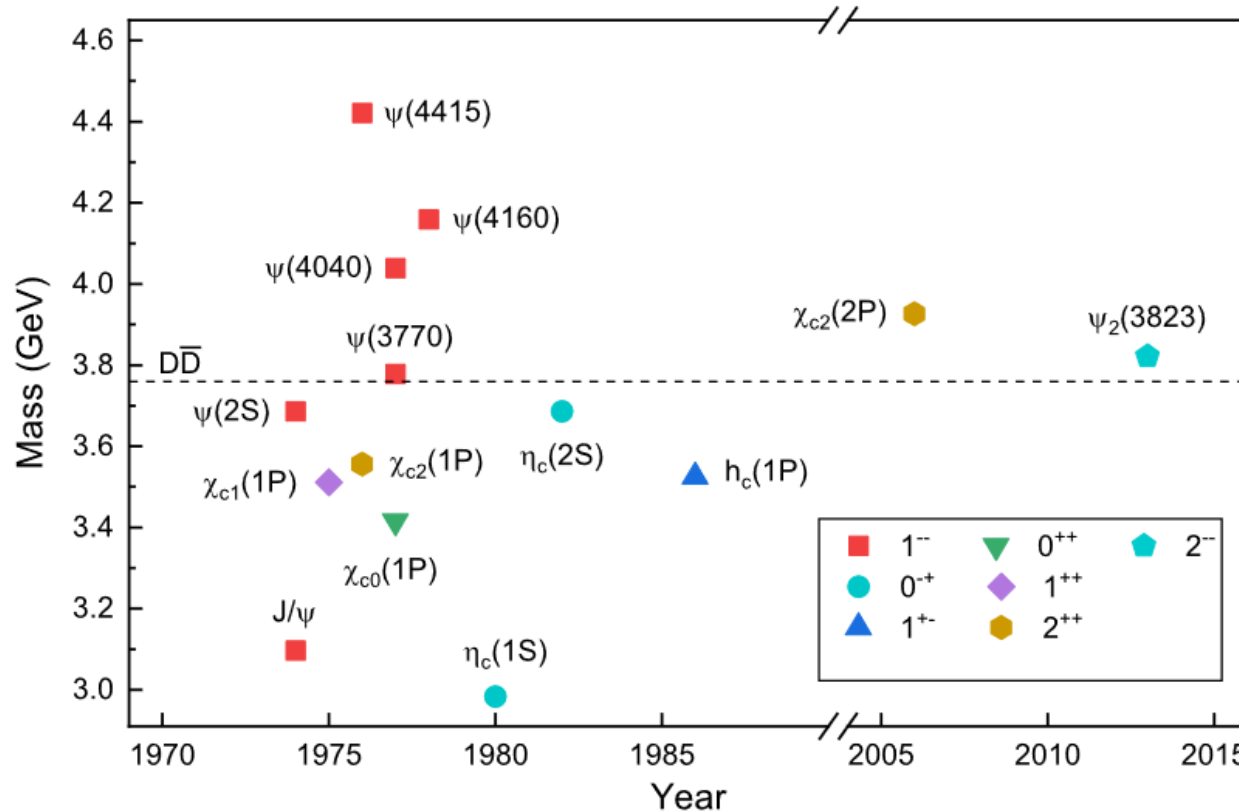


FIG. 1. The observed charmonia with the corresponding first observed year [1,2,4–17]. Here, the  $D\bar{D}$  threshold is also given.

## Charmoniumlike XYZ states

H. X. Chen, W. Chen, X. Liu and S. L. Zhu, The hidden-charm pentaquark and tetraquark states, Phys. Rept. 639, 1 (2016).

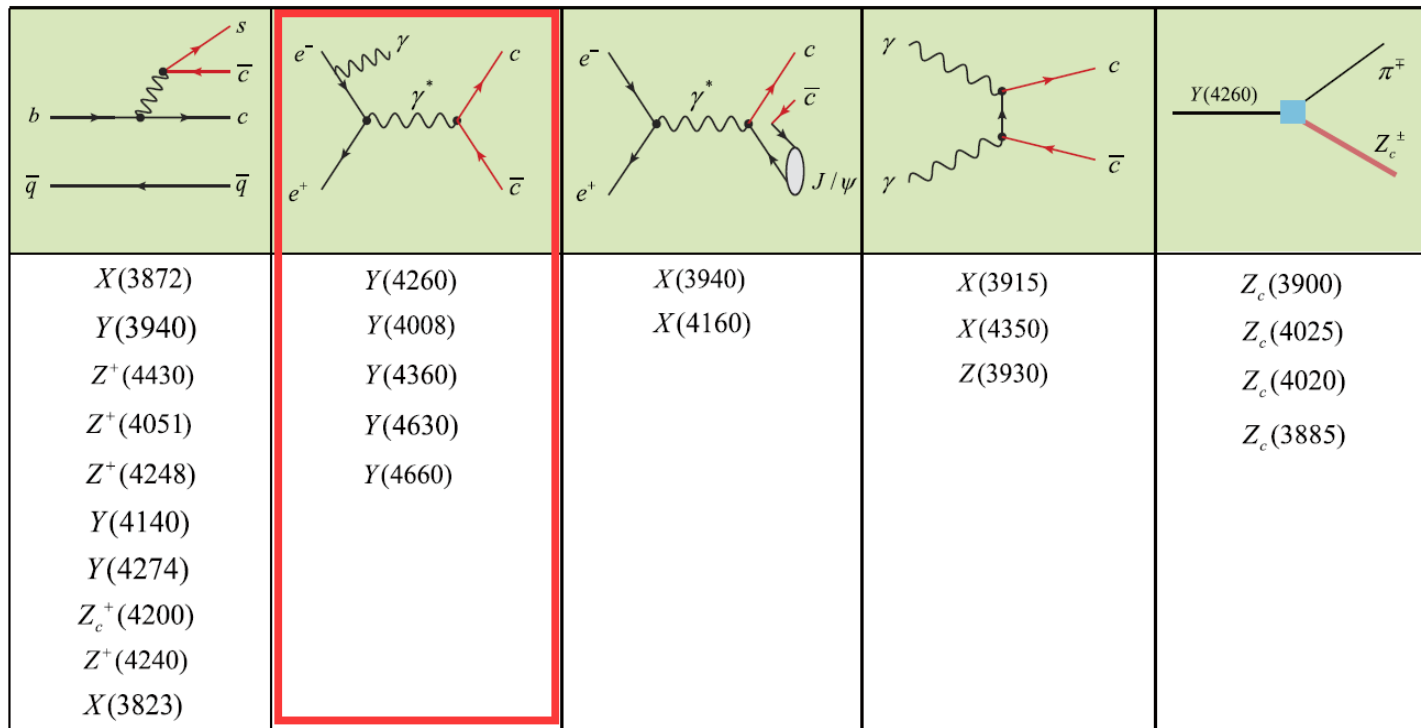
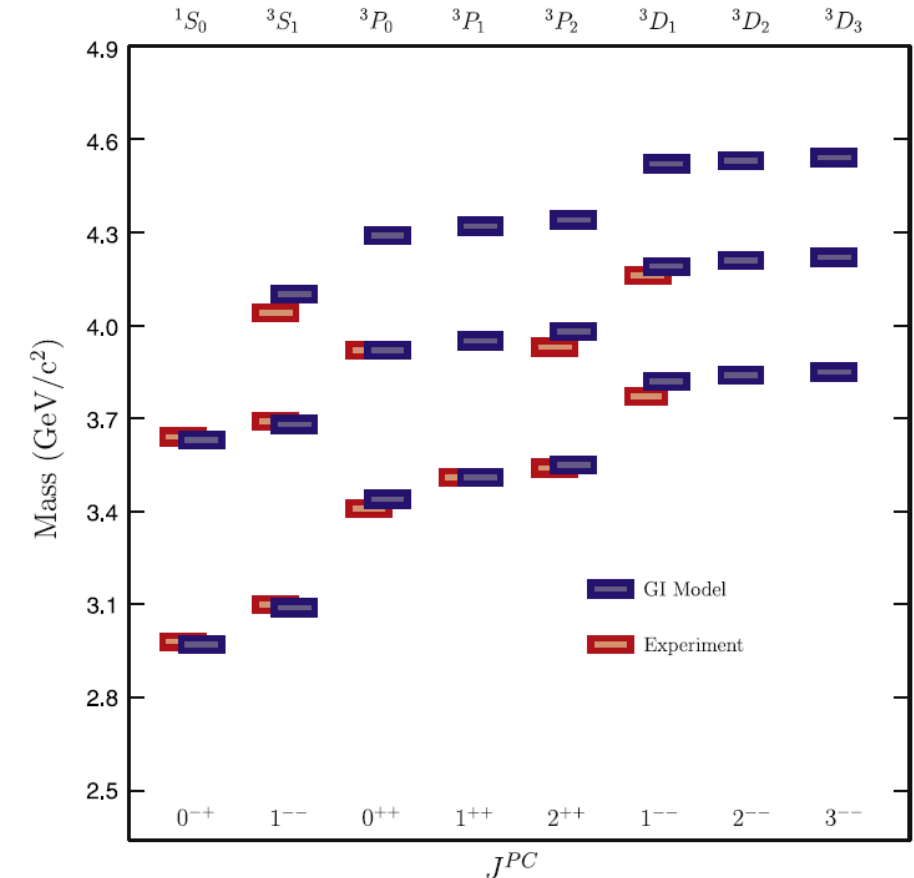
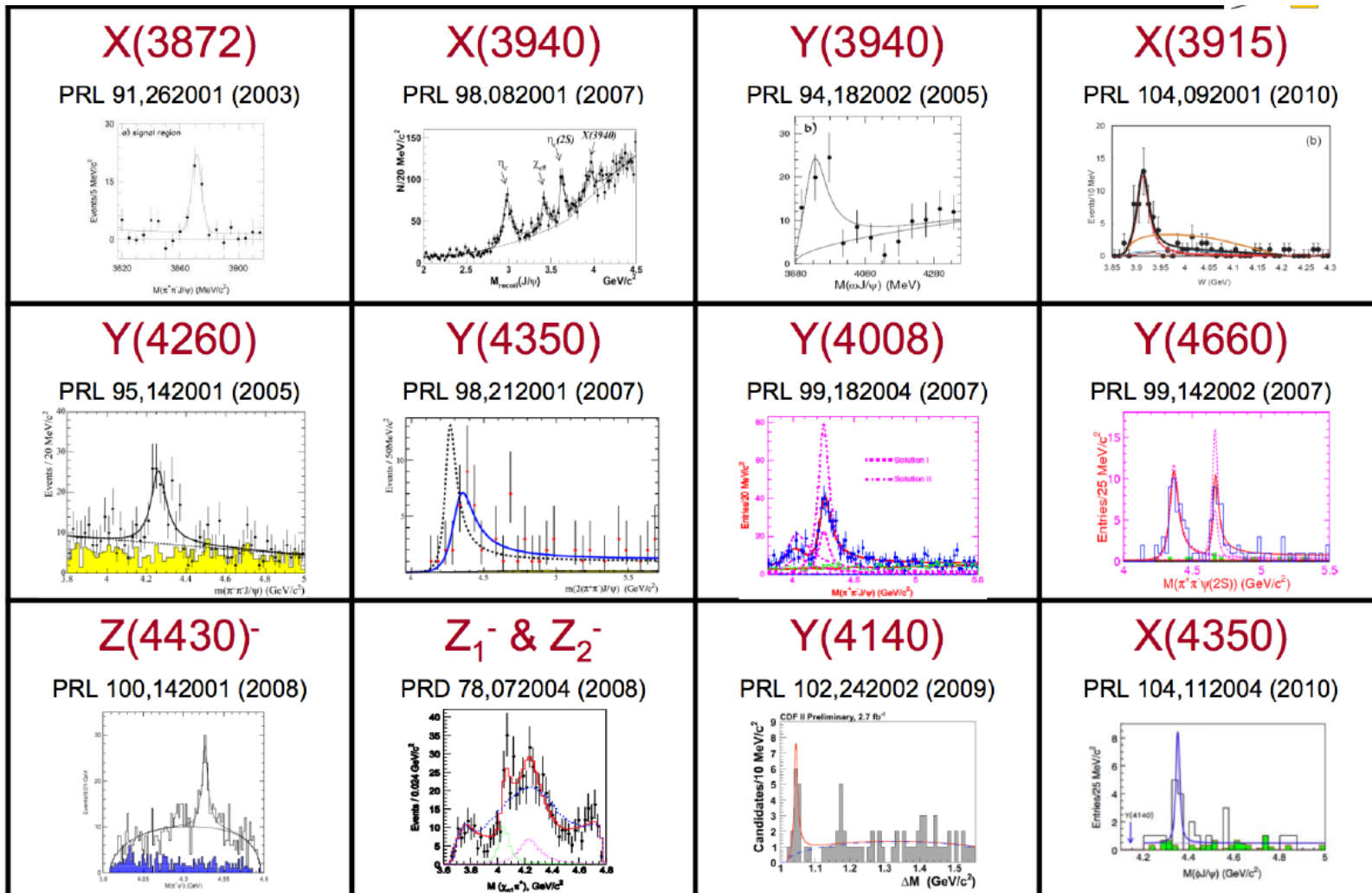


Fig. 2. (Color online) Five groups of the charmonium-like states corresponding to five production mechanisms.

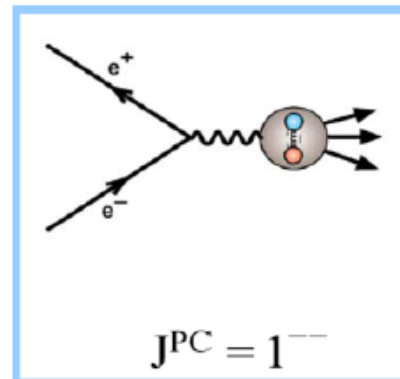


## Some hot Charmoniumlike structures



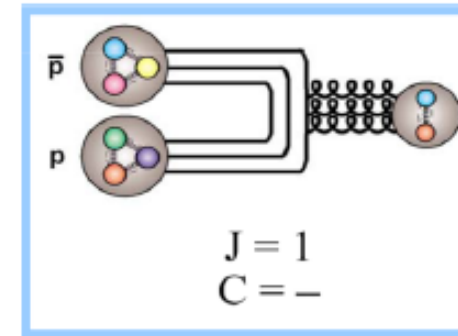
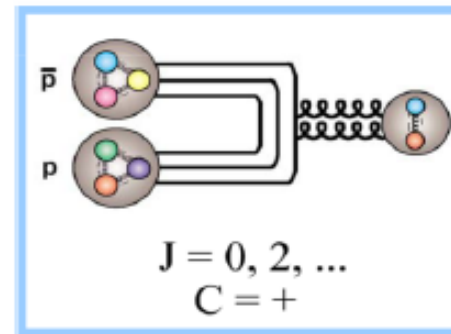
## Advantage of proton-antiproton scattering platform

### Electron-positron platform



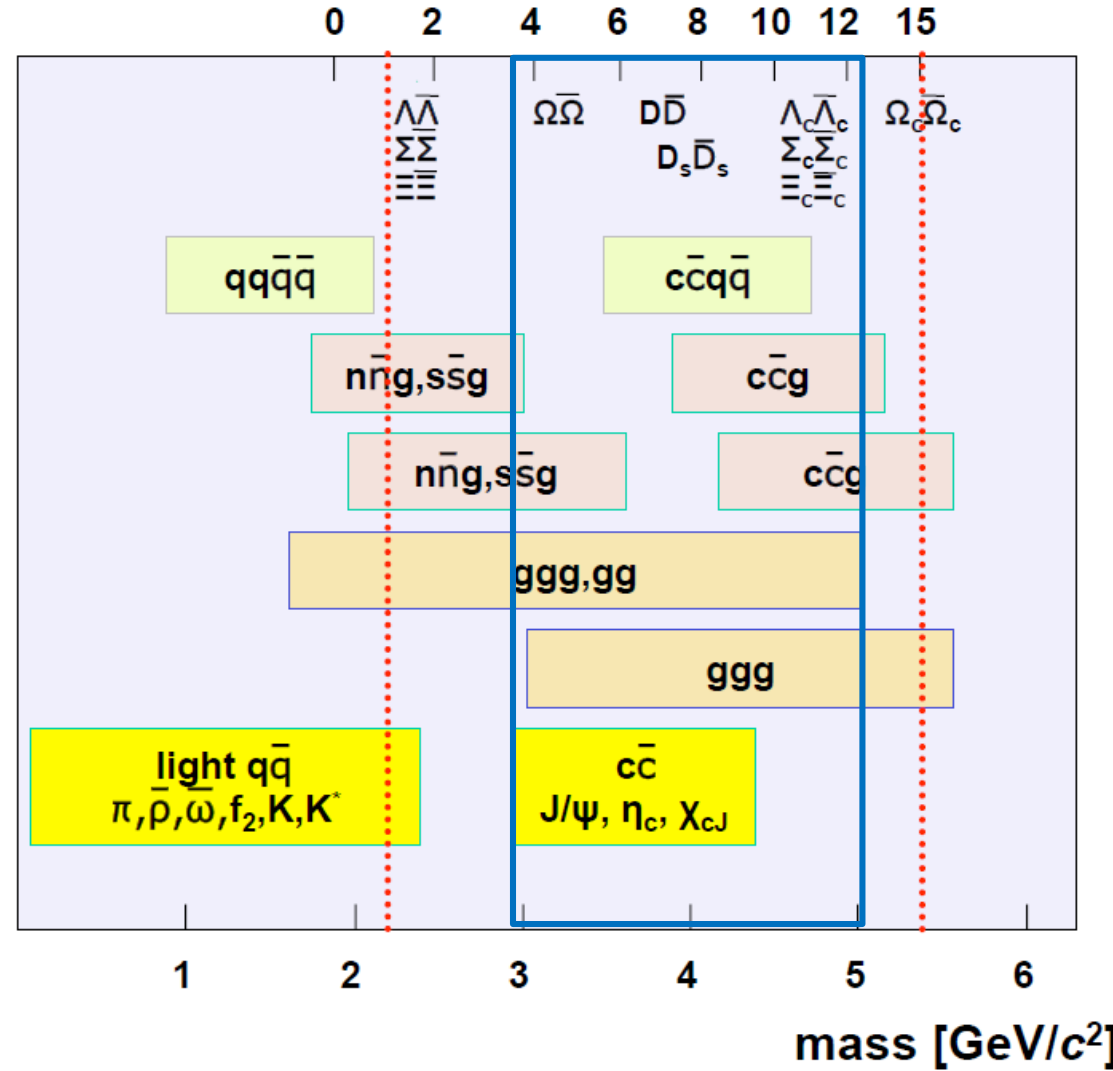
→ Only  $J^{PC} = 1^-$  allowed in  $e^+e^-$

### proton-antiproton platform



→ All  $J^{PC}$  allowed for  $(q\bar{q})$  accessible in  $p\bar{p}$

## PANDA Physics Programme



## Initial state light meson emission model

T.Barnes, X.Li, Phys.Rev.D 75,054018(2007)



FIG. 1. The diagrams describing the production charmonium plus a light meson by the  $p\bar{p}$  interaction. Here,  $\Psi$  denotes charmonium ( $\eta_c, J/\psi, \psi', \chi_{c0}, \chi_{c1}$ ) while  $m$  is light meson ( $\pi^0, \eta, \rho, \omega$ ).

- M. K. Gaillard, L. Maiani and R. Petronzio, Soft Pion Emission in  $p\bar{p}$  Resonance Formation, [Phys. Lett. \*\*110B\*\*, 489 \(1982\)](#).
- A. Lundborg, T. Barnes and U. Wiedner, Charmonium production in  $p\bar{p}$  annihilation: Estimating cross sections from decay widths, [Phys. Rev. D \*\*73\*\*, 096003 \(2006\)](#).
- T. Barnes and X. Li, Associated Charmonium Production in Low Energy  $p\bar{p}$  Annihilation, [Phys. Rev. D \*\*75\*\*, 054018 \(2007\)](#).
- T. Barnes, X. Li and W. Roberts, Evidence for a  $J/\psi p\bar{p}$  Pauli Strong Coupling?, [Phys. Rev. D \*\*77\*\*, 056001 \(2008\)](#).
- T. Barnes, X. Li and W. Roberts, A Meson Emission Model of  $\Psi \rightarrow N\bar{N} m$  Charmonium Strong Decays, [Phys. Rev. D \*\*81\*\*, 034025 \(2010\)](#).
- Q. Y. Lin, H. S. Xu and X. Liu, Revisiting the production of charmonium plus a light meson at PANDA, [Phys. Rev. D \*\*86\*\*, 034007 \(2012\)](#).
- W. H. Liang, P. N. Shen, B. S. Zou and A. Faessler, Nucleon pole contributions in  $J/\psi \rightarrow N\bar{N}\pi$ ,  $p\bar{p}\eta$ ,  $p\bar{p}\eta'$  and  $p\bar{p}\omega$  decays, [Eur. Phys. J. A \*\*21\*\*, 487 \(2004\)](#).
- Y. Y. Zong, P. N. Shen, B. S. Zou, J. F. Liu and W. H. Liang, Re-study of nucleon pole contribution in  $J/\psi \rightarrow N\bar{N}\pi$  decay, [Commun. Theor. Phys. \*\*46\*\*, 507 \(2006\)](#).



## Introduction of the form factor

# Charmonium production in the low energy proton-antiproton collision

PHYSICAL REVIEW D **86**, 034007 (2012)

## Revisiting the production of charmonium plus a light meson at $\bar{\text{P}}\text{ANDA}$

Qing-Yong Lin (林青勇),<sup>1,2,3,\*</sup> Hu-Shan Xu (徐珊瑚),<sup>1,2</sup> and Xiang Liu (刘翔)<sup>4,5,†</sup>

<sup>1</sup>Institute of Modern Physics, Chinese Academy of Sciences, Lanzhou 730000, China

<sup>2</sup>Research Center for Hadron and CSR Physics, Lanzhou University and Institute of Modern Physics of CAS, Lanzhou 730000, China

<sup>3</sup>Graduate University of Chinese Academy of Sciences, Beijing 100049, China

<sup>4</sup>School of Physical Science and Technology, Lanzhou University, Lanzhou 730000, China

<sup>5</sup>Research Center for Hadron and CSR Physics, Lanzhou University and Institute of Modern Physics of CAS, Lanzhou 730000, China

(Received 21 March 2012; published 6 August 2012)

$$\mathcal{L}_{ppm} = \begin{cases} -ig_{NN\pi}\bar{\phi}\gamma_5\tau \cdot \boldsymbol{\pi}\phi, & \text{for } m = \pi^0 \\ -g_{NN\omega}\left(\bar{\phi}\gamma_\mu\phi\omega_\mu - \frac{\kappa_\omega}{4m_p}\bar{\phi}\sigma_{\mu\nu}\phi F_{\mu\nu}\right), & \text{for } m = \omega \end{cases}$$

$$\mathcal{L}_{pp\Psi} = \begin{cases} -ig_{NN\eta_c}\bar{\phi}\gamma_5\phi\eta_c, & \text{for } \Psi = \eta_c \\ -g_{NN\chi_{c0}}\bar{\phi}\phi\chi_{c0}, & \text{for } \Psi = \chi_{c0} \\ -g_{NNJ/\psi(\psi')}\bar{\phi}\gamma_\mu\phi\psi_\mu, & \text{for } \Psi = J/\psi(\psi') \\ -g_{NN\chi_{c1}}\bar{\phi}\gamma_\mu\gamma_5\phi\chi_{c1}^\mu, & \text{for } \Psi = \chi_{c1} \end{cases}$$

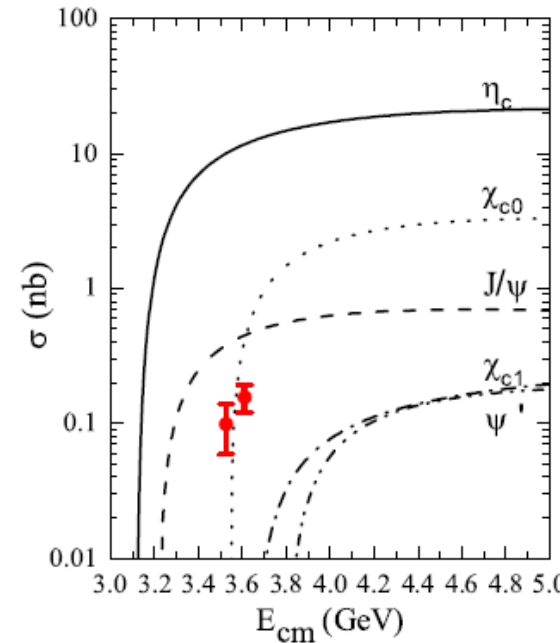
$$\begin{aligned} \mathcal{M}_{\bar{p}p \rightarrow \pi^0\Psi}^{FF} &= g_\pi g_\Psi \bar{v}_{\bar{p}}(p_2, s_2) \\ &\times \left[ \Gamma_1 \frac{(\not{p}_1 - \not{k} + m_p)}{(t - m_p^2)} \gamma^5 \mathcal{F}^2(q_t^2) \right. \\ &\quad \left. + \gamma^5 \frac{(\not{k} - \not{p}_2 + m_p)}{(u - m_p^2)} \Gamma_1 \mathcal{F}^2(q_u^2) \right] u_p(p_1, s_1) \end{aligned}$$

$$\boxed{\mathcal{F}(q_i^2) = (\Lambda^2 - m_i^2)/(\Lambda^2 - q_i^2)}$$

$$\begin{aligned} \mathcal{M}_{\bar{p}p \rightarrow \omega\Psi}^{FF} &= g_\omega g_\Psi \bar{v}_{\bar{p}}(p_2, s_2) \left[ \Gamma_2 \frac{(\not{p}_1 - \not{k} + m_p)}{(t - m_p^2)} \gamma^\mu \mathcal{F}^2(q_t^2) + \gamma^\mu \frac{(\not{k} - \not{p}_2 + m_p)}{(u - m_p^2)} \Gamma_2 \mathcal{F}^2(q_u^2) \right] u_p(p_1, s_1) \epsilon_\mu^* \\ &\quad + i \frac{\kappa_\omega g_\omega g_\Psi}{2m_p} \bar{v}_{\bar{p}}(p_2, s_2) \left[ \Gamma_2 \frac{(\not{p}_1 - \not{k} + m_p)}{(t - m_p^2)} \sigma^{\mu\nu} k_\nu \mathcal{F}^2(q_t^2) + \sigma^{\mu\nu} k_\nu \frac{(\not{k} - \not{p}_2 + m_p)}{(u - m_p^2)} \Gamma_2 \mathcal{F}^2(q_u^2) \right] u_p(p_1, s_1) \epsilon_\mu^*, \end{aligned}$$

## The total cross sections and angular distributions of $p\bar{p} \rightarrow \pi^0\Psi$

Without FF



With FF of  $\Lambda = 1.90$

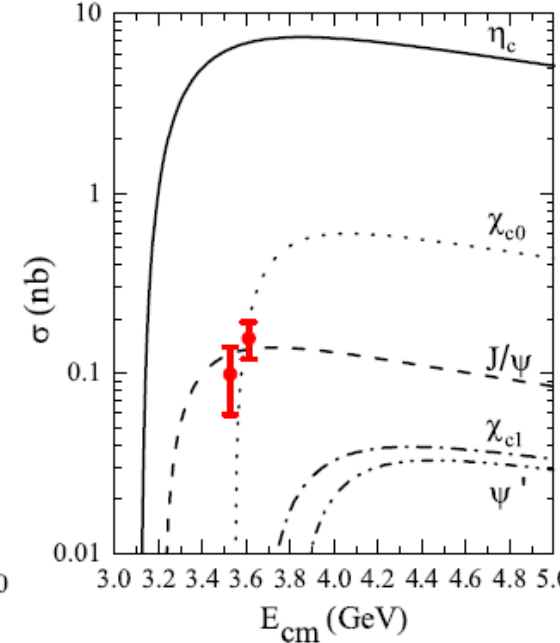


FIG. 2 (color online). The obtained total cross section of  $p\bar{p} \rightarrow \pi^0\Psi$  and the comparison of the experimental and theoretical results. Here, the red points with errors are the experimental measurement from E760 [7]. The left-hand and right-hand diagrams correspond to the theoretical results without and with the FF contribution to  $p\bar{p} \rightarrow \pi^0\Psi$ , respectively.

## The total cross sections and angular distributions of $p\bar{p} \rightarrow \pi^0\Psi$

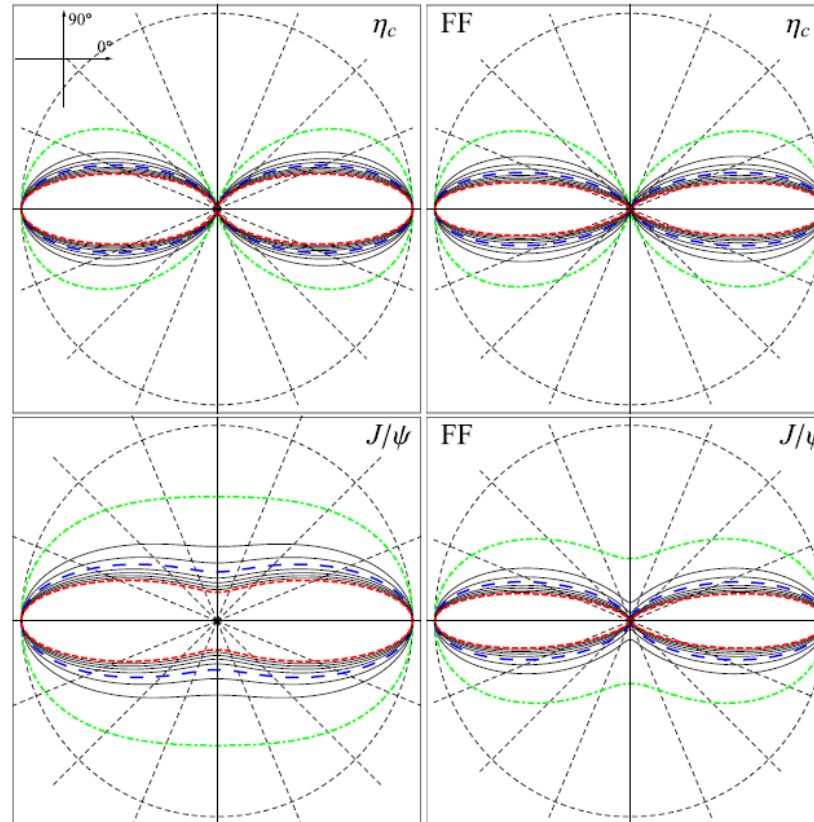


FIG. 4 (color online). The center-of-mass frame angular distribution  $d\sigma/d\Omega$  of  $p\bar{p} \rightarrow \pi^0\eta_c$  and  $p\bar{p} \rightarrow \pi^0J/\psi$ . Here, the results are given by taking the range of  $E_{\text{cm}} = 3.2\text{--}5.0$  GeV or  $3.4\text{--}5.0$  GeV with step of 0.2 GeV for the  $\eta_c$  or  $J/\psi$  production. The diagrams in the first column are the results without FF [8]

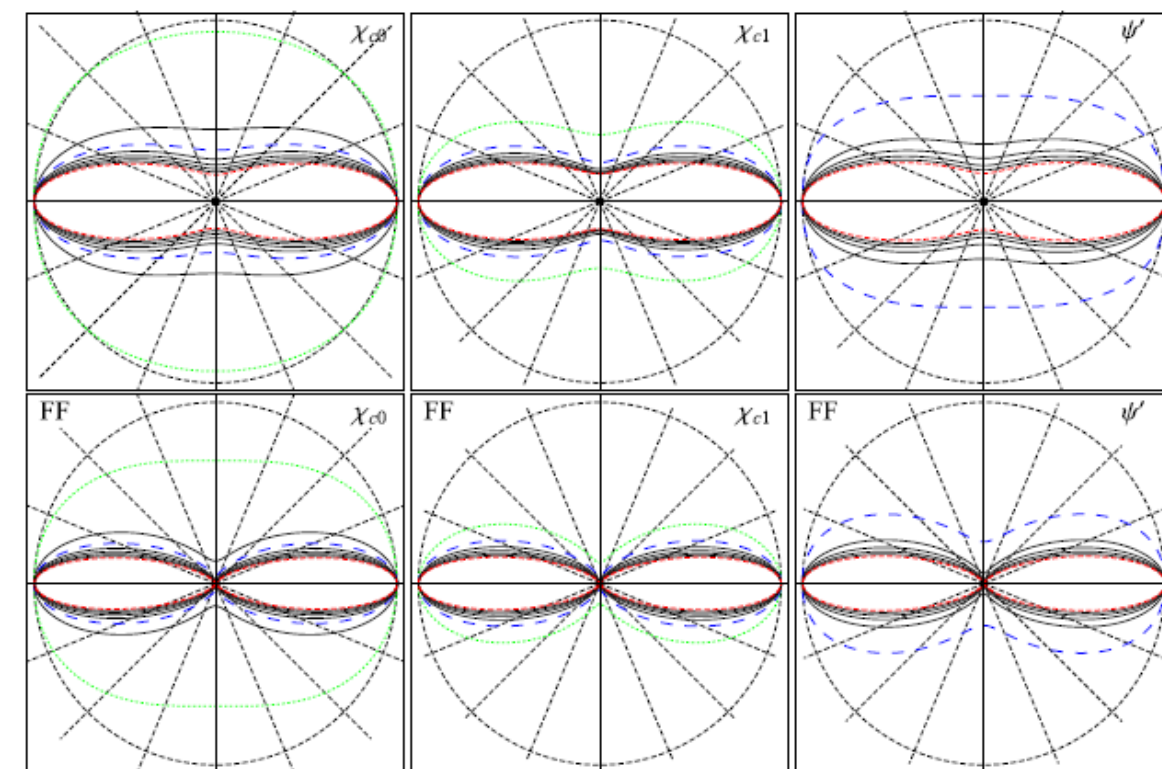


FIG. 5 (color online). The center-of-mass frame angular distribution  $d\sigma/d\Omega$  of  $p\bar{p} \rightarrow \pi^0\chi_{c0}$ ,  $p\bar{p} \rightarrow \pi^0\chi_{c1}$  and  $p\bar{p} \rightarrow \pi^0\psi'$  corresponding to  $E_{\text{cm}} = 3.6\text{--}5.0$  GeV,  $3.8\text{--}5.0$  GeV,  $4.0\text{--}5.0$  GeV with step of 0.2 GeV, respectively. Here, the results without and

## The total cross sections and angular distributions of $p\bar{p} \rightarrow \omega\Psi$ reactions

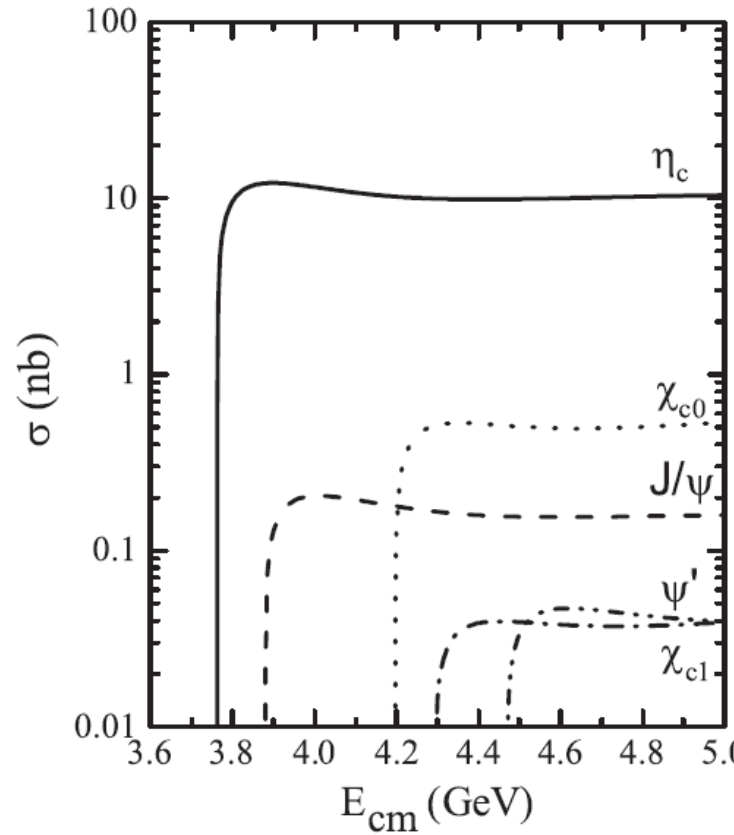


FIG. 7. The predicted total cross sections of  $p\bar{p} \rightarrow \omega\Psi$  corresponding to typical values  $\Lambda = 1.9$  GeV and  $(g_\omega, \kappa_\omega) = (12.2, -0.12)$ .

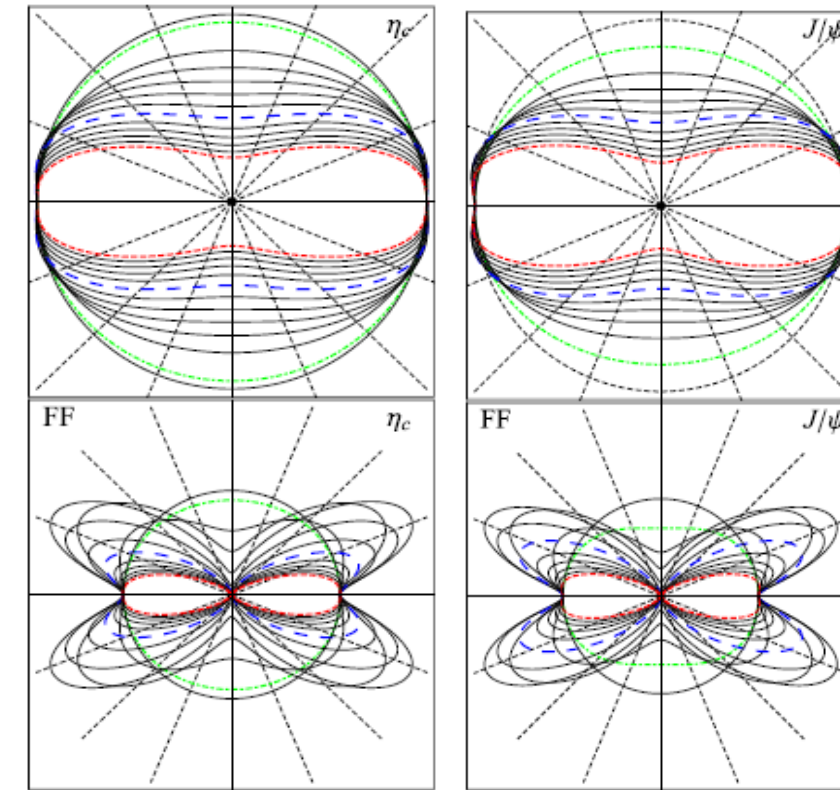


FIG. 8 (color online). The obtained center-of-mass frame angular distribution  $d\sigma/d\Omega$  of  $p\bar{p} \rightarrow \omega\eta_c$  and  $p\bar{p} \rightarrow \omega J/\psi$ . Here, the results are given by taking the range of  $E_{cm} = 3.8\text{--}6.0$  GeV or  $4.0\text{--}6.0$  GeV with step of 0.2 GeV for the  $\eta_c$  or  $J/\psi$  production, respectively. The diagrams in the first and third rows are the results without FF while the remaining diagrams are the results with FF, where we take  $\Lambda = 1.9$  GeV.

## Total cross sections for other processes

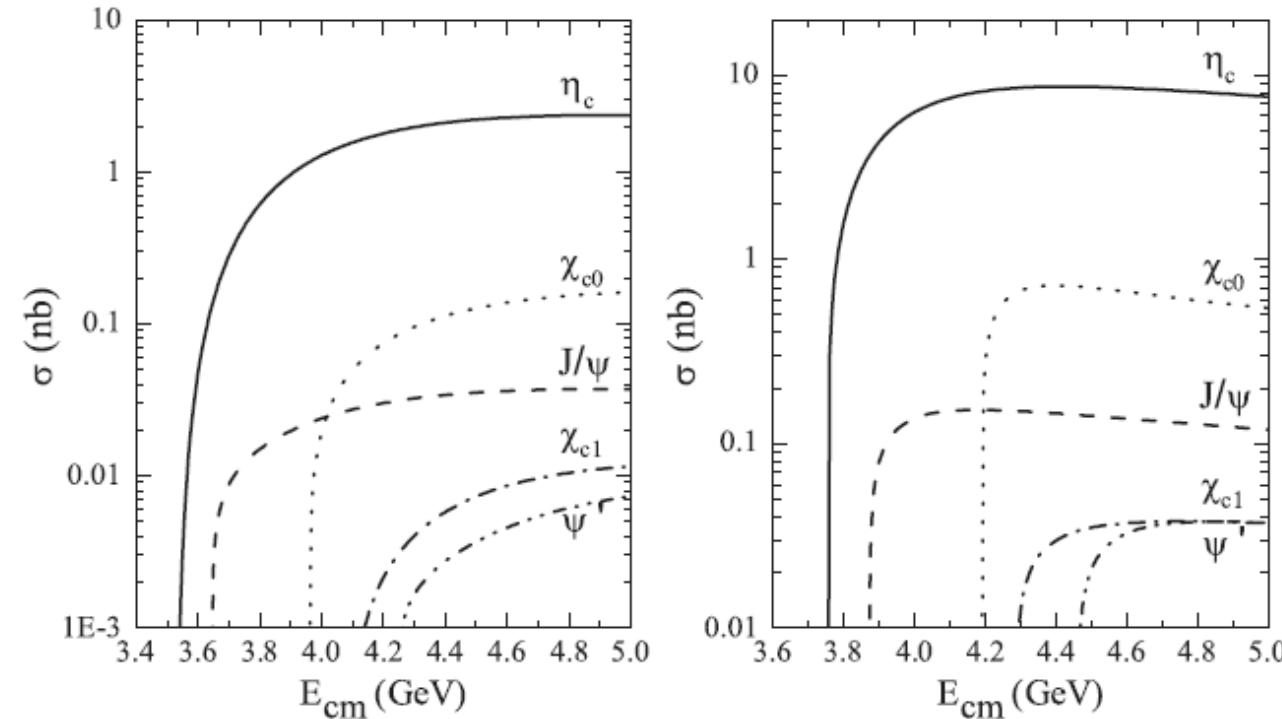
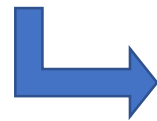


FIG. 9. The total cross sections of the processes  $p\bar{p} \rightarrow \eta\Psi$  (left-hand) and  $p\bar{p} \rightarrow \rho\Psi$  (right-hand) dependent on  $E_{\text{cm}}$ . Here, we take the typical value  $\Lambda = 1.9$  GeV.

## Further improvement of our theoretical predictions

- The uncertainty of cut off parameter in the form factor
- The contributions from exchanging intermediate excited nucleon  $N^*$



**Combining the experimental data of BESIII !**

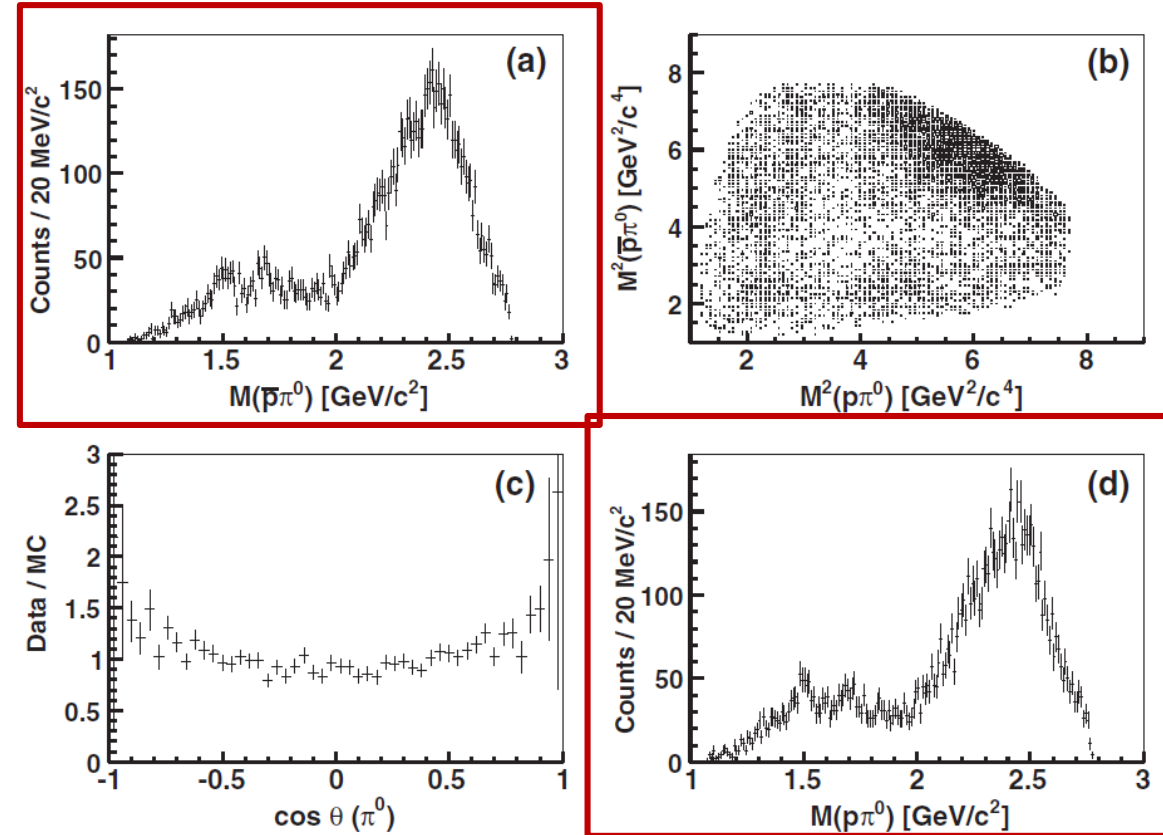
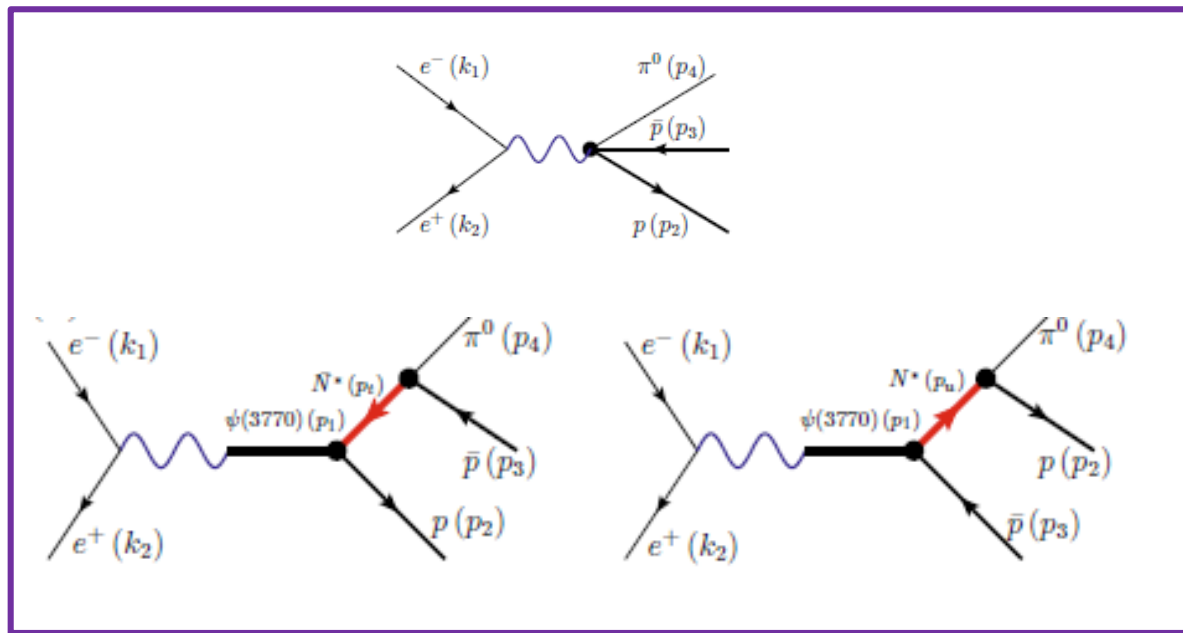
# Predictions of the $p\bar{p} \rightarrow \psi(3770)\pi^0$ and $p\bar{p} \rightarrow \psi(3686)\pi^0$ reaction

PHYSICAL REVIEW D 90, 032007 (2014)

## Study of $e^+e^- \rightarrow p\bar{p}\pi^0$ in the vicinity of the $\psi(3770)$

(BESIII Collaboration)

The process  $e^+e^- \rightarrow p\bar{p}\pi^0$  has been studied by analyzing data collected at  $\sqrt{s} = 3.773$  GeV, at  $\sqrt{s} = 3.650$  GeV, and during a  $\psi(3770)$  line shape scan with the BESIII detector at the BEPCII collider. The Born cross section of  $p\bar{p}\pi^0$  in the vicinity of the  $\psi(3770)$  is measured, and the Born cross section of  $\psi(3770) \rightarrow p\bar{p}\pi^0$  is extracted considering interference between resonant and continuum production amplitudes. Two solutions with the same probability and a significance of  $1.5\sigma$  are found. The solutions for the Born cross section of  $\psi(3770) \rightarrow p\bar{p}\pi^0$  are  $33.8 \pm 1.8 \pm 2.1$  pb and





## Implication of the observed $e^+e^- \rightarrow p\bar{p}\pi^0$ for studying the $p\bar{p} \rightarrow \psi(3770)\pi^0$ process

Hao Xu<sup>1,2,a</sup>, Ju-Jun Xie<sup>1,3,4,b</sup>, Xiang Liu<sup>1,2,4,c</sup>

<sup>1</sup> Research Center for Hadron and CSR Physics, Lanzhou University and Institute of Modern Physics of CAS, Lanzhou 730000, China

<sup>2</sup> School of Physical Science and Technology, Lanzhou University, Lanzhou 730000, China

<sup>3</sup> Institute of Modern Physics, Chinese Academy of Sciences, Lanzhou 730000, China

<sup>4</sup> State Key Laboratory of Theoretical Physics, Institute of Theoretical Physics, Chinese Academy of Sciences, Beijing 100190, China

**Table 1** Relevant resonant parameters for  $N^*$  states

$N^*$	$M_{N^*}$ (MeV)	$\Gamma_{N^*}$ (MeV)
$N(938)$	938	0
$N(1440)$	1430	350
$N(1520)$	1515	115
$N(1535)$	1535	150
$N(1650)$	1655	140
$N(1720)$	1720	250

The values are taken from the Particle Data Book [15]

$$\begin{aligned} \mathcal{M}_{e^+e^- \rightarrow p\bar{p}\pi^0} &= \mathcal{M}_{\text{NoR}} e^{i\phi_{\text{NoR}}} + \bar{v}(k_2) e \gamma^\mu u(k_1) \frac{-g^{\mu\nu}}{s} e m_\psi^2 / f_\psi \\ &\times \frac{-g_{\nu\alpha} + \frac{p_{\psi\nu} p_{\psi\alpha}}{m_\psi^2}}{s - m_\psi^2 + i m_\psi \Gamma_\psi} \left( \mathcal{M}_N^\alpha + \sum_{N^*} \mathcal{M}_{N^*}^\alpha e^{i\phi_{N^*}} \right), \end{aligned}$$

# Predictions of the $p\bar{p} \rightarrow \psi(3770)\pi^0$ and $p\bar{p} \rightarrow \psi(3686)\pi^0$ reaction

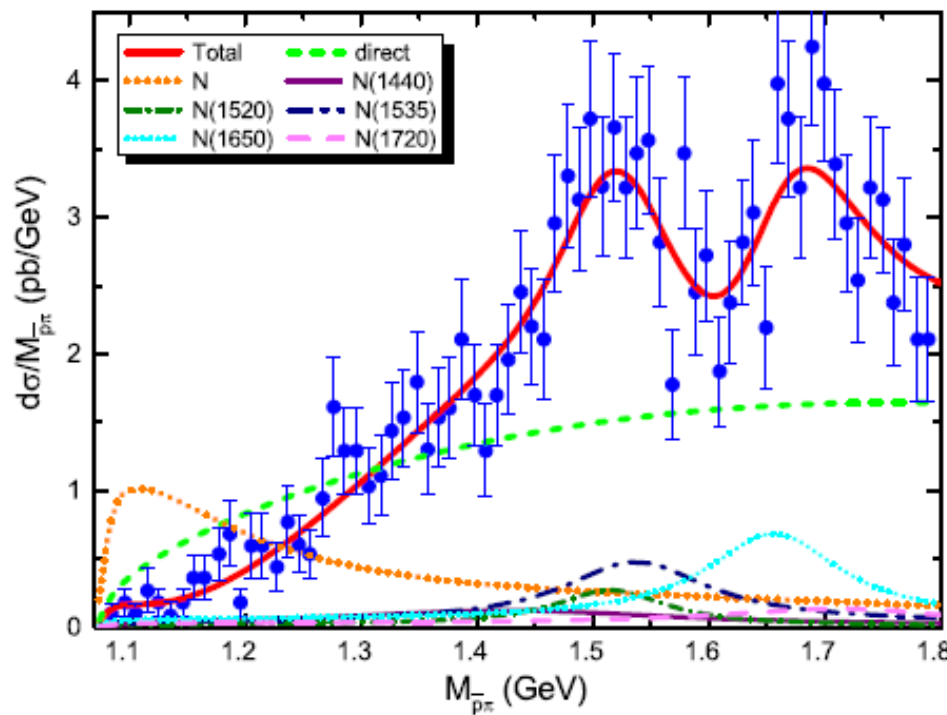


**Fig. 2** (color online) The fitted mass spectrum of the process  $e^+e^- \rightarrow p\bar{p}\pi^0$  at  $\sqrt{s} = 3.773$  GeV comparing to the experiment data. The experiment data are taken from Ref. [10]. The *green dashed line* stands for the background contribution, the *orange dotted line* stands for the nucleon-pole contribution, the *red line* is the full result, and the *other lines* show the contributions from different  $N^*$  resonances. Notice that the experimental event is converted to a physical differential cross section using the experimental total cross section at  $\sqrt{s} = 3.773$  GeV [10]

**Table 2** The fitted parameters in the process  $e^+e^- \rightarrow p\bar{p}\pi^0$ , where  $g_{N^*} = g_{\psi(3770)NN^*}g_{\pi NN^*}$

$N^*$	$g_{N^*} (\times 10^{-3})$	$\phi_{N^*}$ (rad)
$N(938)$	$8.00 \pm 0.46$	–
$N(1440)$	$1.92 \pm 0.98$	$6.09 \pm 0.38$
$N(1520)$	$0.28 \pm 0.24$	$3.74 \pm 1.07$
$N(1535)$	$1.74 \pm 1.34$	$2.99 \pm 0.67$
$N(1650)$	$1.99 \pm 0.18$	$2.17 \pm 0.19$
$N(1720)$	$1.14 \pm 0.63$	$6.02 \pm 0.71$

For nucleon,  $g_N$  is defined as  $g_N = g_{\psi(3770)NN}g_{\pi NN}$

$$F(q^2) = \frac{\Lambda^4}{\Lambda^4 + (q^2 - M_{N^*}^2)^2},$$

$$\beta = 6.2 \pm 3.5.$$

# Predictions of the $p\bar{p} \rightarrow \psi(3770)\pi^0$ and $p\bar{p} \rightarrow \psi(3686)\pi^0$ reaction

## The total cross section of $p\bar{p} \rightarrow \psi(3770)\pi^0$

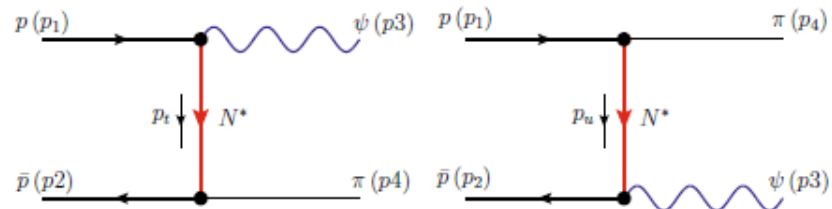


Fig. 3 (color online) The typical Feynman diagrams for the process  $p\bar{p} \rightarrow \pi^0 \psi(3770)$

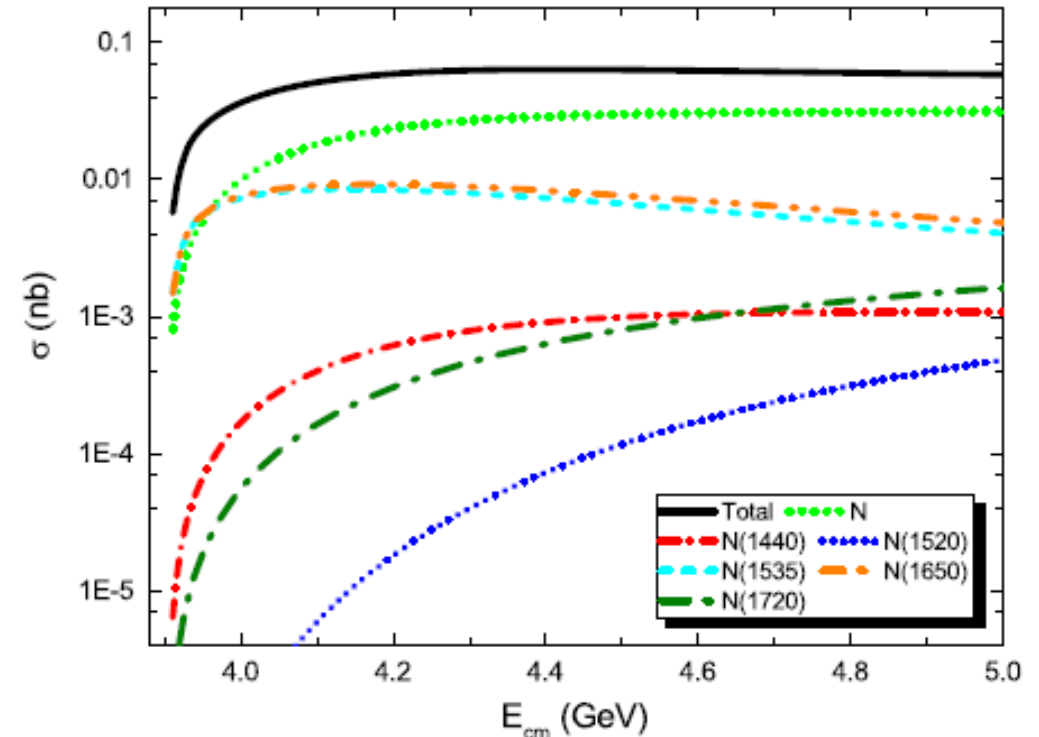


Fig. 4 (color online) Total cross section of the  $p\bar{p} \rightarrow \pi^0 \psi(3770)$  reaction. The *black line* is the total result, and the *other lines* show the contributions from different  $N^*$  resonances

# Predictions of the $p\bar{p} \rightarrow \psi(3770)\pi^0$ and $p\bar{p} \rightarrow \psi(3686)\pi^0$ reaction

## The angular distributions of $p\bar{p} \rightarrow \psi(3770)\pi^0$

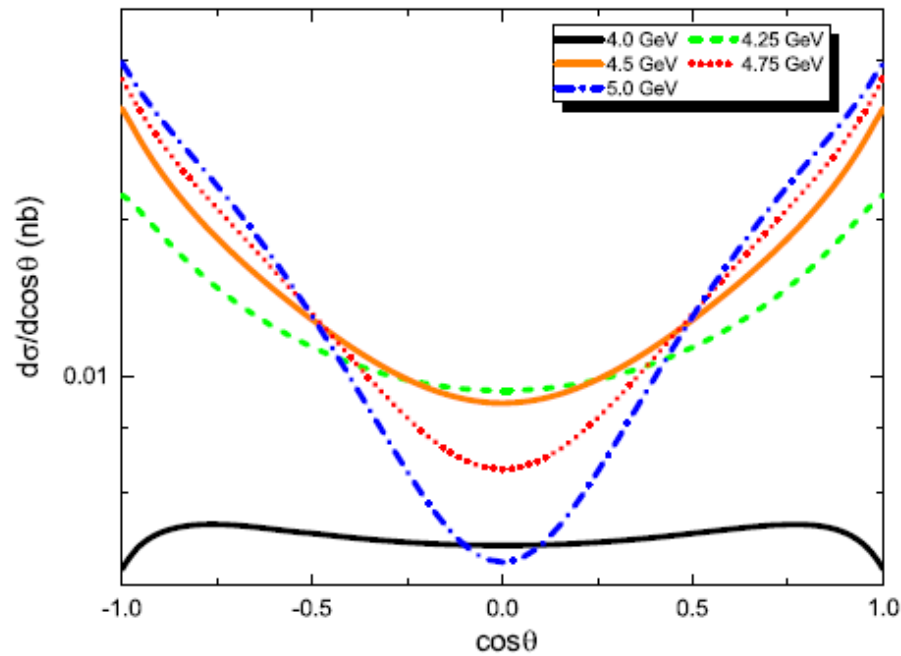


Fig. 6 (color online) Angular distributions of the  $p\bar{p} \rightarrow \pi^0\psi(3770)$  reaction considered only the contribution from the nucleon pole

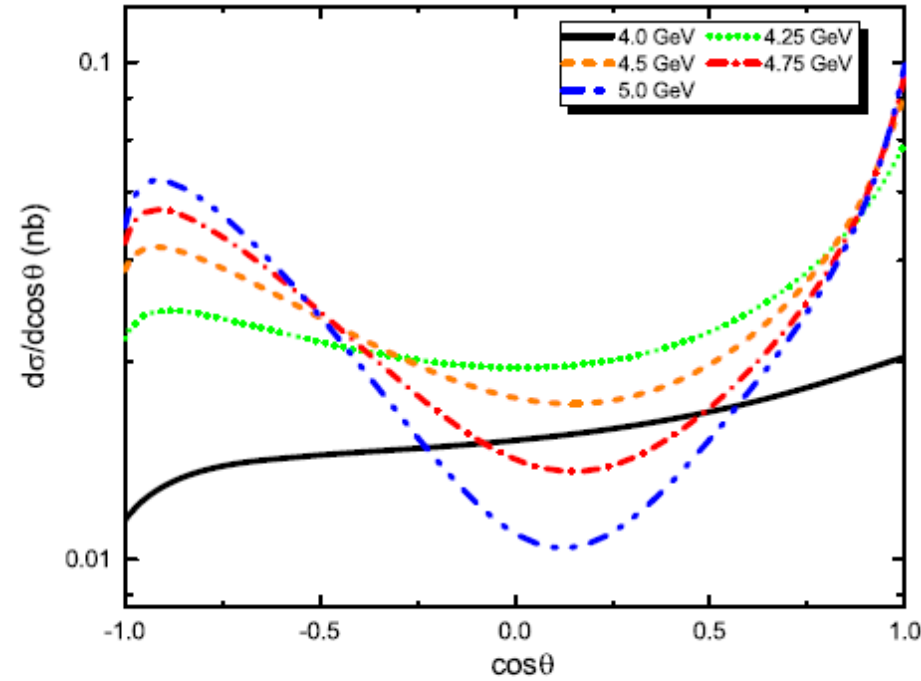


Fig. 5 (color online) Angular distributions of the  $p\bar{p} \rightarrow \pi^0\psi(3770)$  reaction with full contribution

# Predictions of the $p\bar{p} \rightarrow \psi(3770)\pi^0$ and $p\bar{p} \rightarrow \psi(3686)\pi^0$ reaction

The results of  $p\bar{p} \rightarrow \psi(3686)\pi^0$

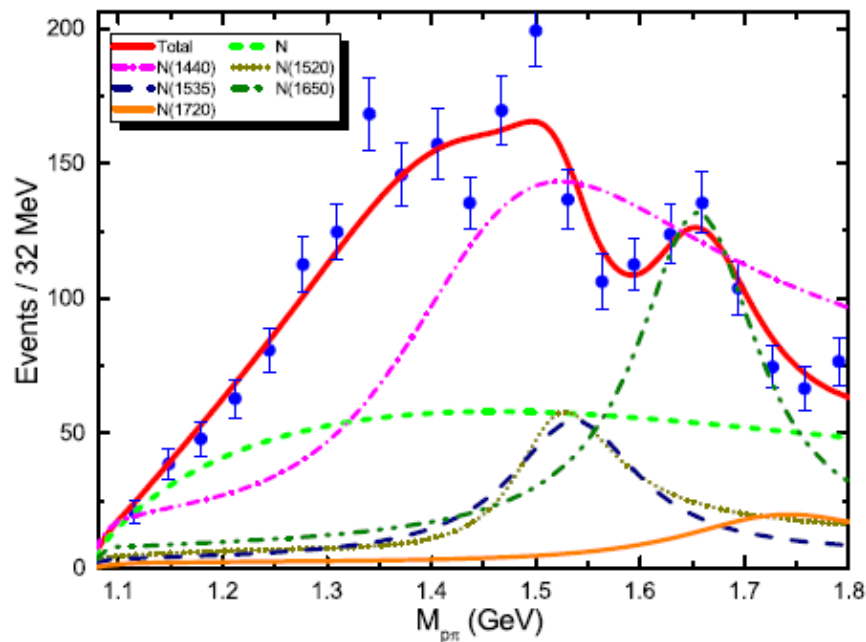


Fig. 7 (color online) The fitted  $p\pi$  invariant mass spectrum of the process of  $\psi(3686) \rightarrow p\bar{p}\pi^0$ . The *dashed green curve* stands for the contribution of the nucleon pole, the *solid red line* stands for the full contributions, and the *other lines* show the contributions from different  $N^*$  resonances. The experiment data are taken from Ref. [14]

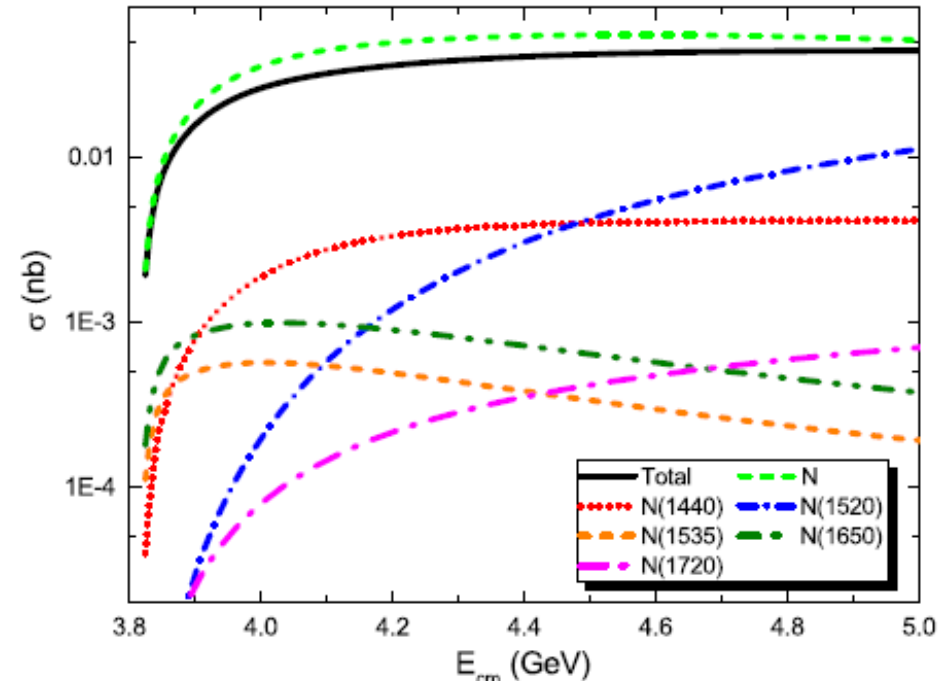


Fig. 8 (color online) The cross section of the process  $p\bar{p} \rightarrow \pi^0\psi(3686)$ . The *black line* is total result, and the *other lines* show the  $N^*$  contribution

# Predictions of the $p\bar{p} \rightarrow \psi(3770)\pi^0$ and $p\bar{p} \rightarrow \psi(3686)\pi^0$ reaction

## The results of $p\bar{p} \rightarrow \psi(3686)\pi^0$

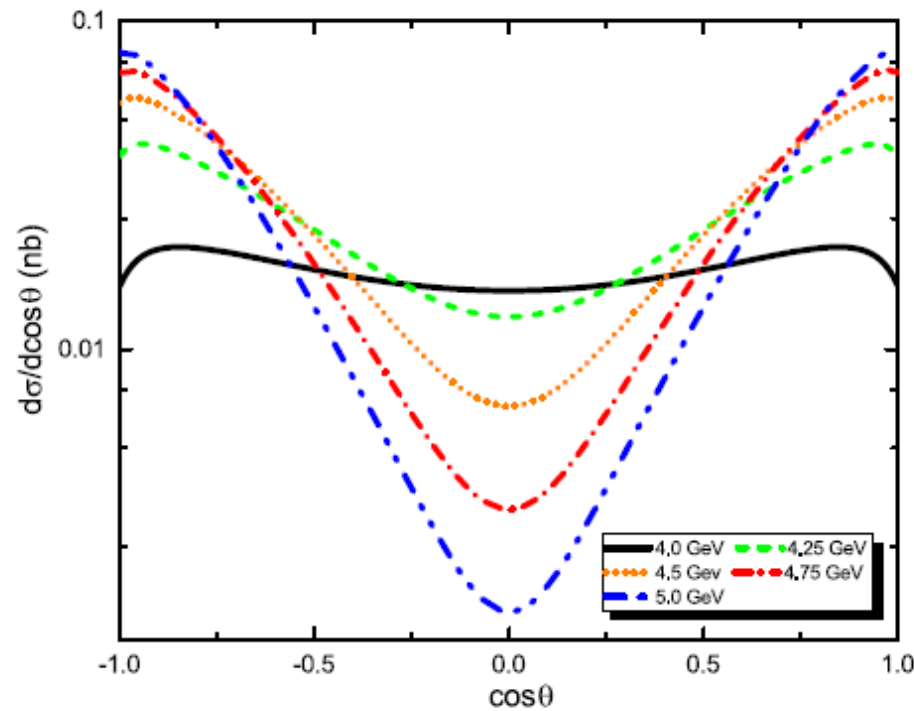


Fig. 10 (color online) The angular distribution of the process  $p\bar{p} \rightarrow \pi^0\psi(3686)$  only considering the nucleon contribution. Each line shows a different c.m. energy

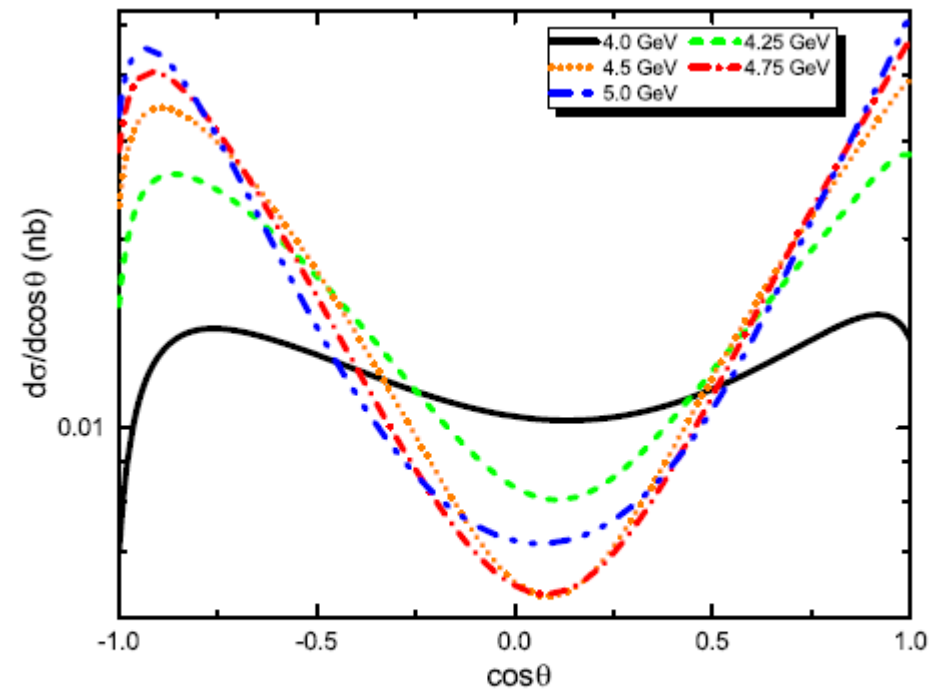
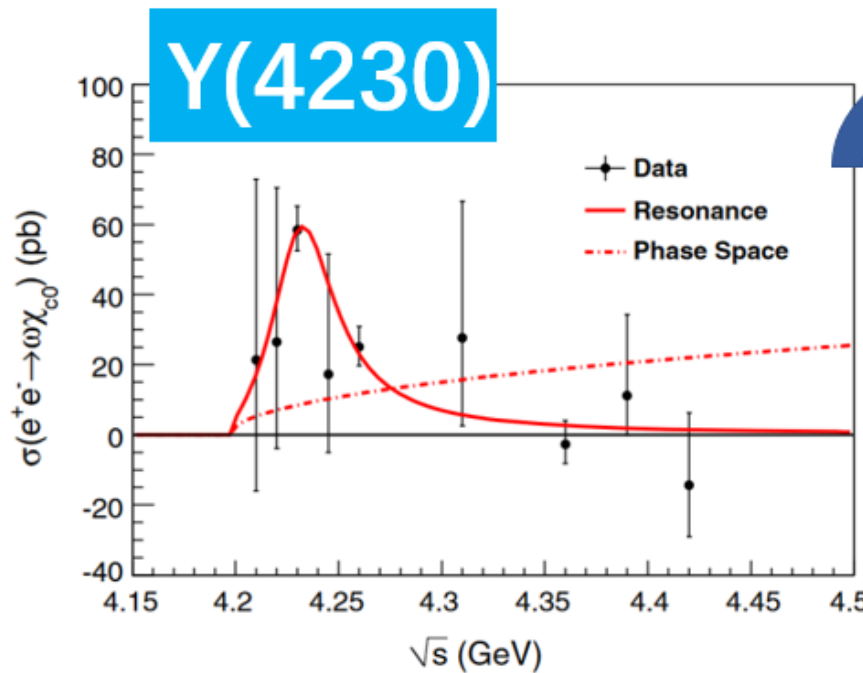


Fig. 9 (color online) The angular distribution of the process  $p\bar{p} \rightarrow \pi^0\psi(3686)$ . Each line shows a different c.m. energy

# Measurements of $e^+e^- \rightarrow \chi_{c0}\omega$ from the BESIII

This structure is confirmed by the precise data in 2019 !

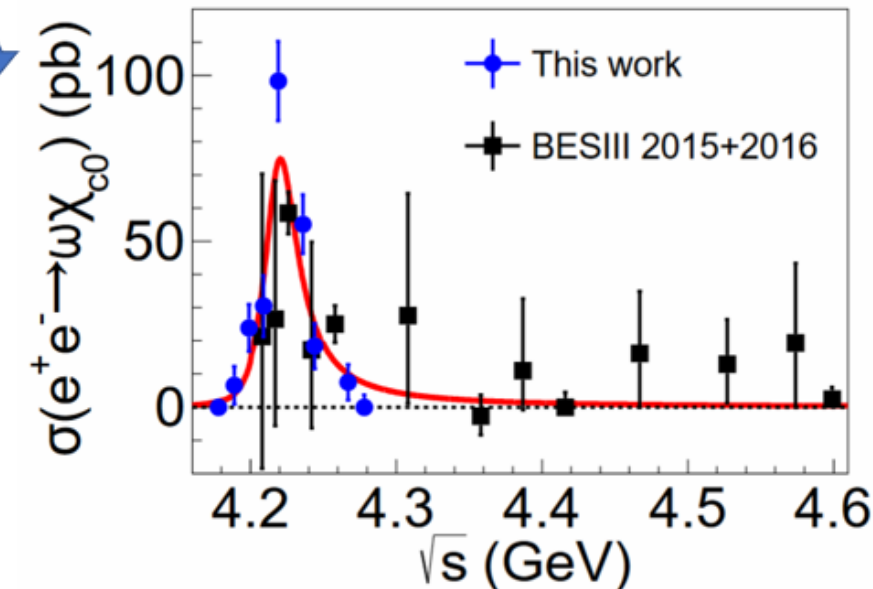


PRL 114,092003 (2015)

## Resonance parameters

$$M = (4218.5 \pm 1.6(\text{stat.}) \pm 4.0(\text{sys.})) \text{ MeV}/c^2$$

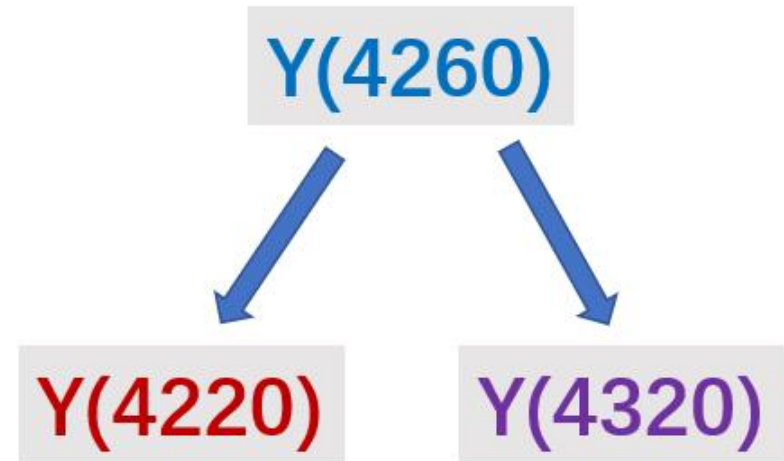
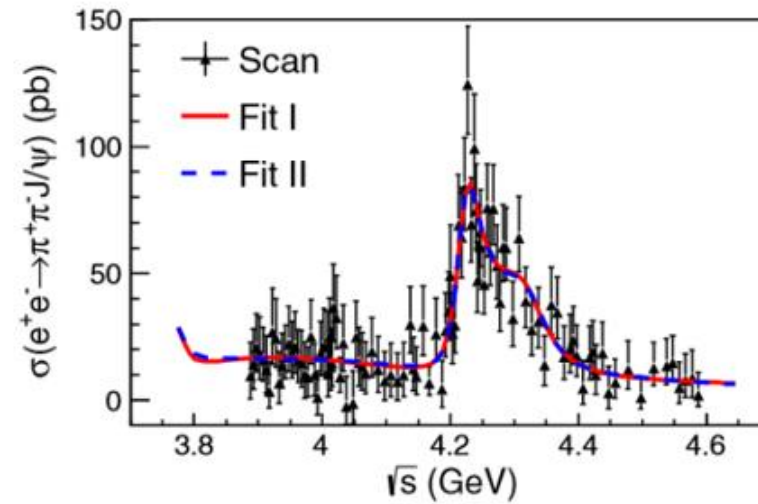
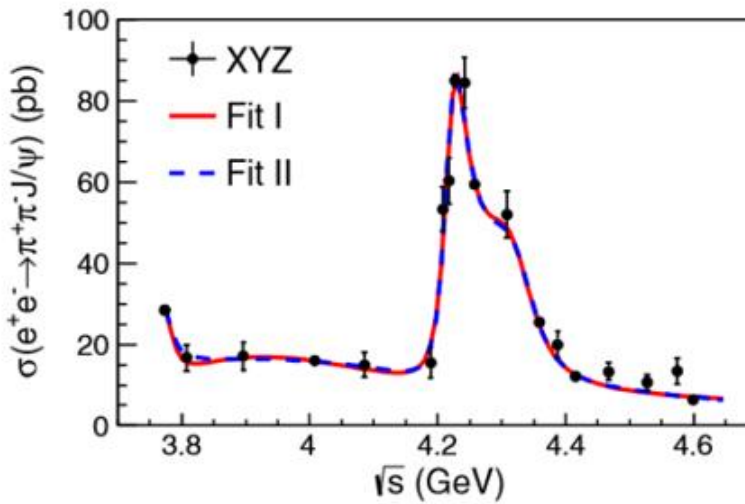
$$\Gamma = (28.2 \pm 3.9(\text{stat.}) \pm 1.6(\text{sys.})) \text{ MeV}$$



Phys.Rev. D99 (2019) no.9, 091103

## Measurements of $e^+e^- \rightarrow J/\psi \pi^+ \pi^-$ from the BESIII

PRL 118, 092001 (2017)

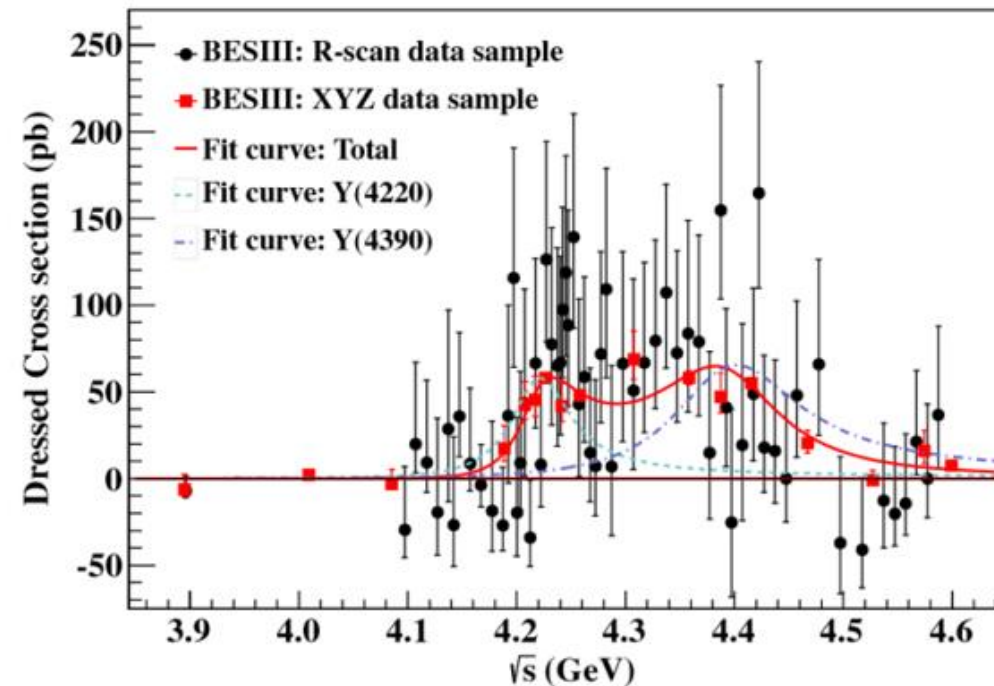


The resonant parameters:  $M(Y(4220)) = (4222.0 \pm 3.1 \pm 1.4)$  MeV,  $\Gamma(Y(4220)) = (44.1 \pm 4.3 \pm 2.0)$  MeV,  
 $M(Y(4320)) = (4320.0 \pm 10.4 \pm 7.0)$  MeV,  $\Gamma(Y(4320)) = (101.4^{+25.3}_{-19.7} \pm 10.2)$  MeV.

## Measurements of $e^+e^- \rightarrow h_c\pi^+\pi^-$ from the BESIII

Y(4220)

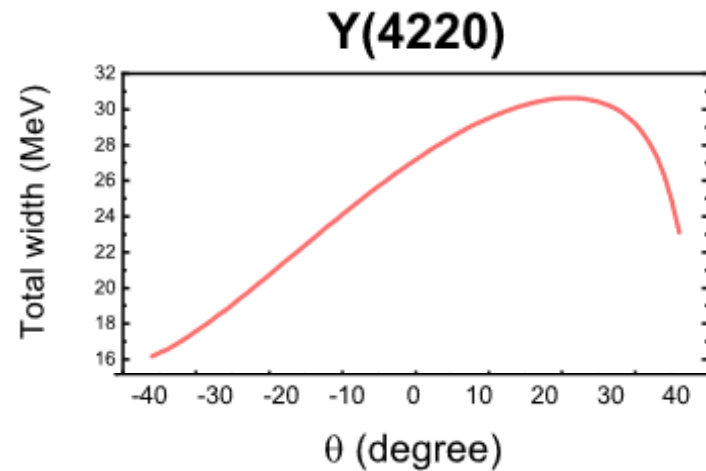
Y(4390)



PRL 118, 092002 (2017)

The resonant parameters:  $M(Y(4220)) = (4218.4^{+5.5}_{-4.5} \pm 0.9)$  MeV,  $\Gamma(Y(4220)) = (66.0^{+12.3}_{-8.3} \pm 0.4)$  MeV,  
 $M(Y(4390)) = (4391.5^{+6.3}_{-6.8} \pm 1.0)$  MeV,  $\Gamma(Y(4390)) = (139.5^{+16.2}_{-20.6} \pm 0.6)$  MeV.

# Predictions of the $p\bar{p} \rightarrow Y(4220)\pi^0$ reaction



B.-Q.Li, K.-T.Chao, Phys.Rev.D 79,094004 (2009).

Y.B.Dong, Y.W.Yu, Z.Y.Zhang, P.N.Shen, Phys.Rev.D 49,1642 (1994).

Eur. Phys. J. C 74,no.12,3208 (2014)

Physical Review D 91,094023 (2015)

J.Z.Wang, D.Y.Chen, X.Liu and T.Matsuki,  
Phys.Rev.D 99, no.11,114003 (2019)

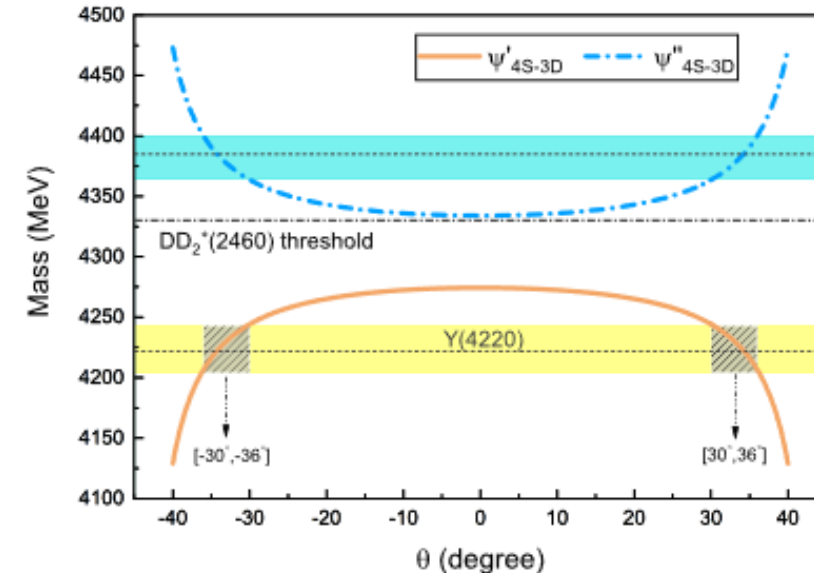
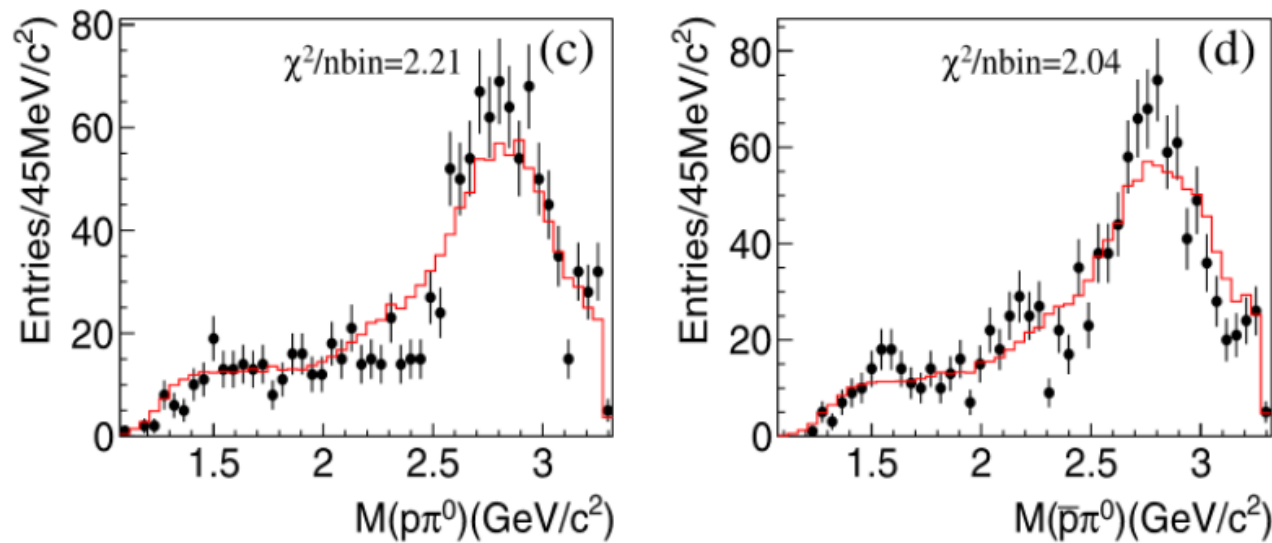


FIG. 5: The masses of  $\psi'_{4S-3D}$  and  $\psi''_{4S-3D}$  with dependence on the  $4S-3D$  mixing angle  $\theta$ . The yellow and cyan bands denote the measured mass range of  $Y(4220)$  and the predicted mass range of  $\psi(4380)$ , respectively, where the dashed horizontal lines in bands corresponds to each average value. The two shaded regions represent the mixing angle interval, in which the theoretical results of  $\psi'_{4S-3D}$  meet the measurements of  $Y(4220)$ .

Support that  $Y(4220)$  is missing charmonium  $\Psi(4S)$ .

# Predictions of the $p\bar{p} \rightarrow Y(4220)\pi^0$ reaction

- The study of  $Y(4220)$  state in different production processes supplies useful information on their properties, and PANDA experiment is an ideal platform.
- In 2017, BESIII released the measurements of  $e^+e^- \rightarrow p\bar{p}\pi^0$  at center-of-mass energies between 4.008 to 4.600 GeV, which provide an excellent opportunity to fix the information of  $Y(4220)$ . [Phys.Lett. B771 (2017) 45-51]



**Figure 5:** Invariant mass spectra of  $p\pi$  and  $\bar{p}\pi$  at  $\sqrt{s}=4.258$  GeV.

# Predictions of the $p\bar{p} \rightarrow Y(4220)\pi^0$ reaction

Phys.Rev. D96 (2017) no.9, 094004 [ in collaboration with Hao. Xu, Ju.Jun. Xie and Xiang. Liu ].

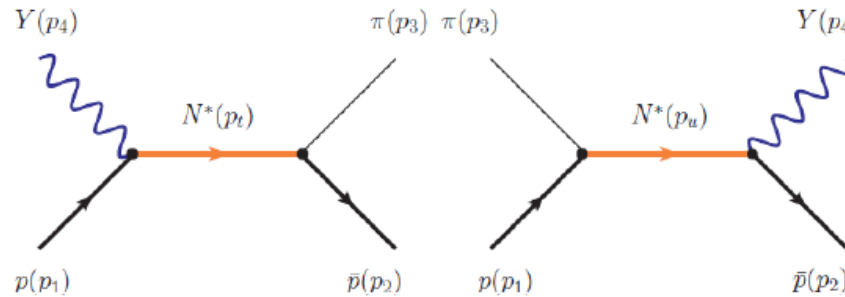


FIG. 1: The Feynman diagrams describing the process  $p\bar{p} \rightarrow Y(4220)\pi^0$ . Left:  $t$ -channel exchange; Right:  $u$ -channel exchange. The  $Y$  stands for the  $Y(4220)$  state and  $N^*$  represents nucleon pole and the excited nuclear resonances.

$$\mathcal{L}_{\pi NN} = -\frac{g_{\pi NN}}{2m_N} \bar{N} \gamma_5 \gamma_\mu \tau \cdot \partial^\mu \pi N,$$

$$\mathcal{L}_{\pi NP_{11}} = -\frac{g_{\pi NP_{11}}}{2m_N} \bar{N} \gamma_5 \gamma_\mu \tau \cdot \partial^\mu \pi R_{P_{11}} + h.c.,$$

$$\mathcal{L}_{\pi NS_{11}} = -g_{\pi NS_{11}} \bar{N} \tau \cdot \pi R_{S_{11}} + h.c.,$$

$$\mathcal{L}_{\pi NP_{13}} = -\frac{g_{\pi NP_{13}}}{m_N} \bar{N} \tau \cdot \partial_\mu \pi R_{P_{13}}^\mu + h.c.,$$

$$\mathcal{L}_{\pi ND_{13}} = -\frac{g_{\pi ND_{13}}}{m_N^2} \bar{N} \gamma_5 \gamma^\mu \tau \cdot \partial_\mu \partial_\nu \pi R_{D_{13}}^\nu + h.c.,$$

$$\mathcal{L}_{YNN} = -g_{YNN} \bar{N} \gamma_\mu V^\mu N,$$

$$\mathcal{L}_{YNP_{11}} = -g_{YNP_{11}} \bar{N} \gamma_\mu V^\mu R_{P_{11}} + h.c.,$$

$$\mathcal{L}_{YNS_{11}} = -g_{YNS_{11}} \bar{N} \gamma_5 \gamma_\mu V^\mu R_{S_{11}} + h.c.,$$

$$\mathcal{L}_{YNP_{13}} = -i g_{YNP_{13}} \bar{N} \gamma_5 V_\mu R_{P_{13}}^\mu + h.c.,$$

$$\mathcal{L}_{YND_{13}} = -g_{YND_{13}} \bar{N} V_\mu R_{D_{13}}^\mu + h.c.,$$

# Predictions of the $p\bar{p} \rightarrow Y(4220)\pi^0$ reaction

- $g_{Nor} = 0.87 \pm 0.34$ ,  $a = 0.646 \pm 0.026$  and  $\beta = 6.74 \pm 3.46$  with  $\chi^2/d.o.f = 0.66$
- Coupling constants of  $g_{N^*} = g_{Y(4220)NN^*} \times g_{\pi NN^*}$  are shown

$N^*$	$J^P$	$m_{N^*}$ (MeV)	$\Gamma_{N^*}$ (MeV)	$g_{N^*} (\times 10^{-3})$
$N(938)$	$\frac{1}{2}^+$	938	0	$66.55 \pm 13.14$
$N(1440)$	$\frac{1}{2}^+$	1430	350	$28.13 \pm 11.42$
$N(1520)$	$\frac{3}{2}^-$	1515	115	$13.72 \pm 3.90$
$N(1535)$	$\frac{1}{2}^-$	1535	150	$2.44 \pm 1.30$
$N(1650)$	$\frac{1}{2}^-$	1655	140	$1.60 \pm 0.88$
$N(1720)$	$\frac{3}{2}^+$	1720	250	$1.72 \pm 0.72$

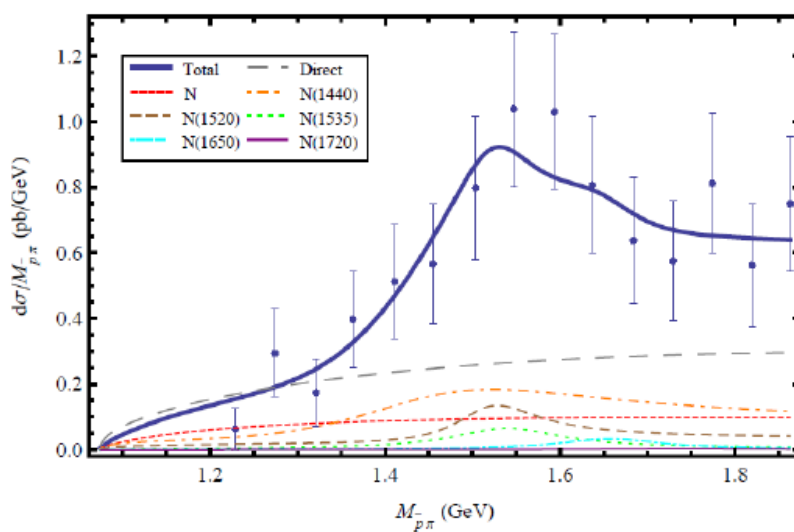


**Figure 6:** Fitting invariant mass spectra of  $\bar{p}\pi$  at  $\sqrt{s}=4.258$  GeV.

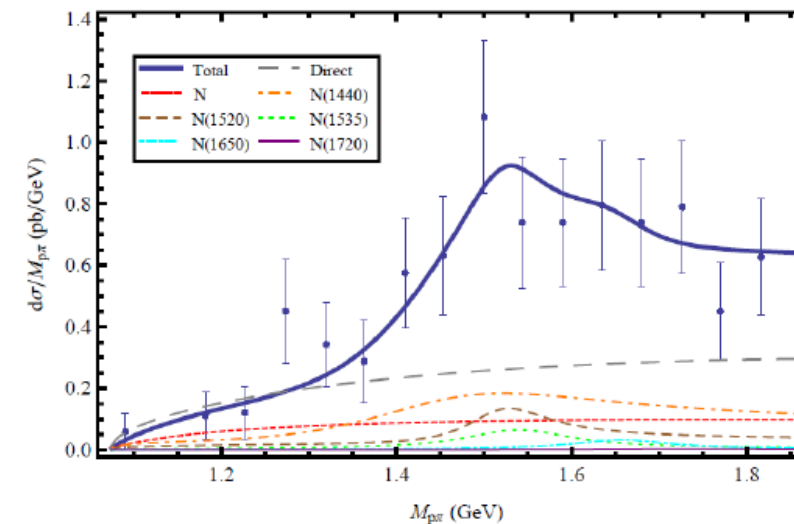


**Figure 7:** Fitting invariant mass spectra of  $p\pi$  at  $\sqrt{s}=4.258$  GeV.

# Predictions of the $p\bar{p} \rightarrow Y(4220)\pi^0$ reaction

The total cross section and angular distributions  
of  $p\bar{p} \rightarrow Y(4220)\pi^0$

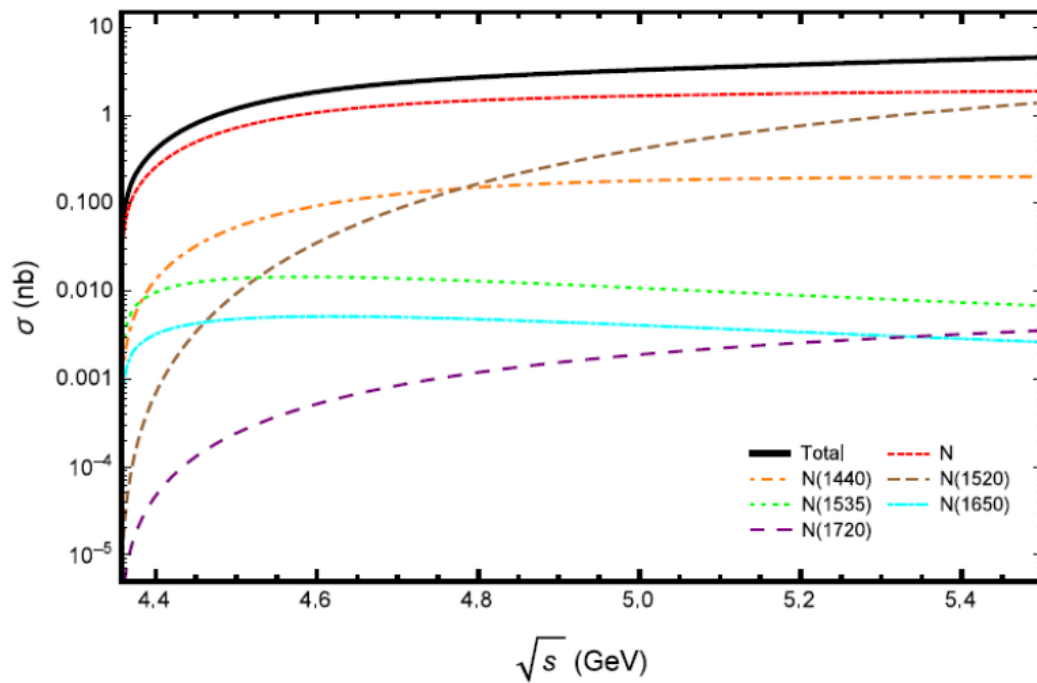


FIG. 4: The total cross sections of  $p\bar{p} \rightarrow Y(4220)\pi^0$  as a function of  $\sqrt{s}$ .

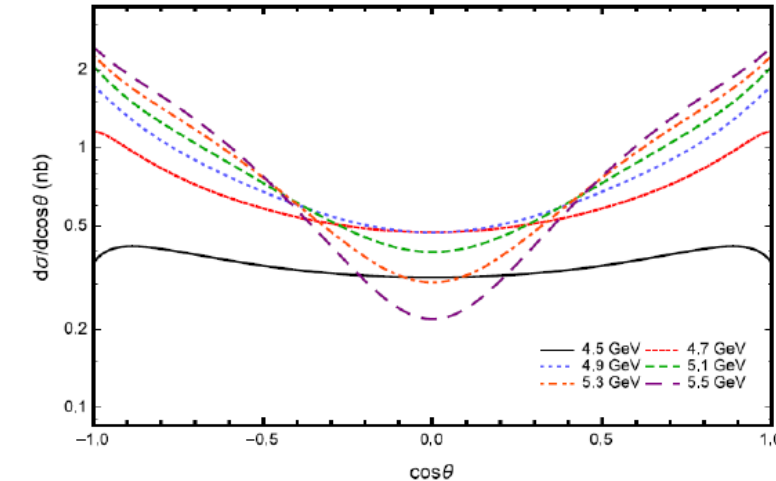


FIG. 6: The angular distributions of  $p\bar{p} \rightarrow Y(4220)\pi^0$  with the contributions from the nucleon pole alone.

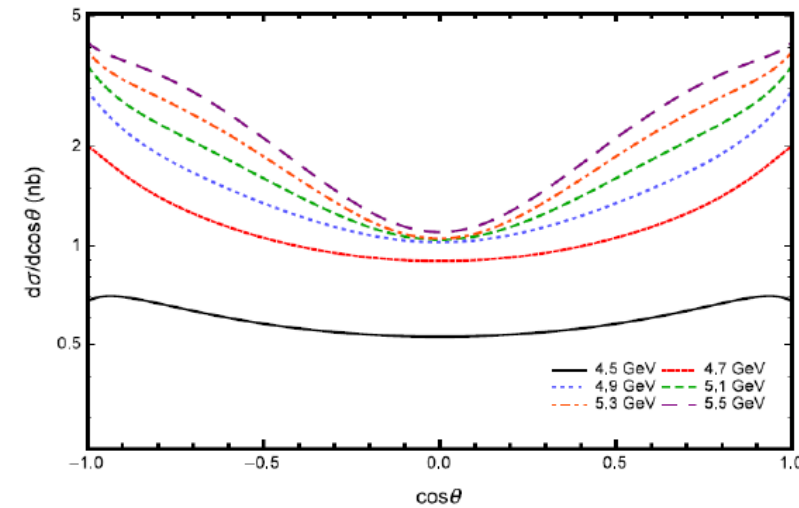


FIG. 5: The angular distributions of  $p\bar{p} \rightarrow Y(4220)\pi^0$  with the contributions from both nucleon pole and excited nucleon resonances.

# **Thanks for your attention!**